Superficies y Vacío **17(1)**, 1-6, marzo de 2004
©Sociedad Mexicana de Ciencia de Superficies y de Vacío

Photoluminescence in off-stoichiometric silicon oxide compounds

Z. Yu*, M. Aceves
INAOE Apdo 51, Puebla, Pue. 72000 México

J. Carrillo, F. Flores
CIDS-ICUAP, Universidad Autónoma de Puebla, México

C. Falcony
Depto. de Física, CINVESTAV-IPN, México

C. Domínguez, A. Llobera
IMB-CNM (CSIC), 08193-Bellaterra, España

A. Morales-Acevedo
Depto. de Ingenieria Electrica, CINVESTAV-IPN, Mexico
(Recibido 15 de diciembre de 2002; Aceptado 13 de febrero de 2004)

The photoluminescence properties of silicon rich oxide (SRO) and silicon oxynitride (SNO) films were studied. The materials were obtained by the low pressure chemical vapor deposition (LPCVD) technique, with some samples post-treated by Si-implantation and thermal annealing under different conditions. For SRO films, strong red emission with peak at 1.7 eV was observed after Si-implantation and thermal annealing. The emission intensity depends on the deposition and post-treatment parameters. For SNO films, however, strong blue emission with a peak at 2.38-2.66 eV was observed both in the as-deposited and annealed states. The emission intensity and peak position can be adjusted by thermal annealing. This emission band was also compared with that produced by PECVD-SRO films. The experimental results were explained according to the structural properties of each material. It could be possible that the emission depends not only on Si excess but also on the microstructure of the material.

Keywords: Silicon rich oxide; Silicon oxynitride; Photoluminescence; Si excess
PACS codes: 68.35.Dv; 68.55.Ln; 68.35.-P

1. Introduction

In the last years, the interest for the optical properties of the silicon nanocrystals has grown due to its potential applications in optoelectronics [1, 2]. The interest increased when visible luminescence in silicon rich oxide (SRO) was observed [3]. Intense studies have been performed in order to find the origin of the visible light luminescence [4-6] although it is still controversial. However, some possible applications of this material have been proposed [1, 2]. It is thus important to continue studying the luminescence of this material, or other materials containing Si nanocrystals, in order to improve and better understand the light emission properties. In this study, we investigate the photoluminescence of silicon rich oxide (SRO) and silicon oxynitride (SNO) films. It was found that the photoluminescence is sensitive to the preparation parameters of the materials. Strong red and blue light emission can be produced by SRO and SNO, respectively, under proper fabrication conditions.

2. Experiments

Low-pressure chemical vapor deposition (LPCVD) technique was used to deposit both the SRO and SNO films. For the deposition of SRO, gas mixture of SiH_4 and N_2O was used and the excess Si content can be adjusted by changing the gas flow ratio Ro=$[N_2O]/[SiH_4]$. Three gas flow ratio of Ro=10, 20 and 30 were used, and the Si excess will decrease with increasing Ro. For the deposition of SNO films, gas mixture of SiH_4, N_2O and NH_3 was used.

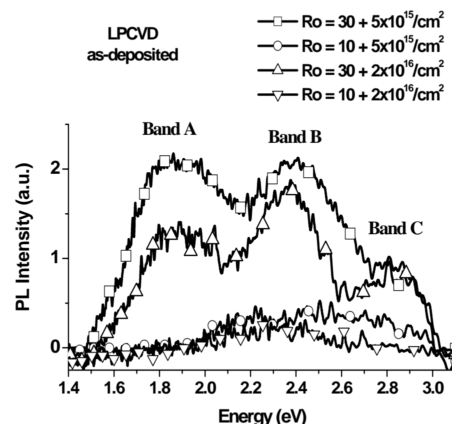

Figure 1. Photoluminescence spectra of as-implanted LPCVD-SRO films.

*zyu@inaoep.mx

Table 1. List of samples and their deposition parameters.

	Name	Ro	R1	R2	Si-implantation
LPCVD-SRO films	SRO10	10	x	x	$5x10^{15}$ (cm^{-2}) $2x10^{16}$ (cm^{-2})
	SRO20	20	x	x	$5x10^{15}$ (cm^{-2}) $2x10^{16}$ (cm^{-2})
	SRO30	30	x	x	$5x10^{15}$ (cm^{-2}) $2x10^{16}$ (cm^{-2})
LPCVD-SNO films	M1	1.0	0.5	0.5	x
	M2	1.0	1.0	1.0	x
	M3	1.0	1.875	1.875	x
	M4	1.0	3.75	3.75	x

We defined the gas flow ratios as Ro=$[N_2O]/[SiH_4]$, R_1=$[SiH_4]/[NH_3]$ and R_2=$[N_2O]/NH_3]$, respectively. During the deposition, Ro was fixed at Ro=1.0 while the composition of SNO films can be changed by adjusting R_1 and R_2. Our previous study with Auger Electron Spectroscopy (not published yet) has shown that the Si excess will increase with increasing R1; and N content will decrease with increasing R2. This has also been observed by other groups [7, 8]. The deposition temperature was 700°C, and pressure varied from 1.9 to 2.5 Torr. The thickness for both SRO and SNO is around 550 nm. In table 1, the experimental parameters of each sample used in this study are listed.

Si-implantation was performed for the SRO films. Two implantation doses, $5x10^{15}$ cm^{-2} and $2x10^{16}$ cm^{-2}, were used at 150 keV for each deposited SRO films. Thermal annealing at 1100°C in N_2 atmosphere was then performed for 30, 60, and 180 min, respectively. For the SNO films, the as-deposited films were thermally annealed at 1000°C in N_2 atmosphere for 45, 90 and 180 min., respectively. Photoluminescence measurements were performed for each sample in the as-deposited state and after thermal annealing.

3. Results

3.1 Photoluminescence of SRO films

Figure 1 shows photoluminescence spectra of SRO_{10} and SRO_{30} (index is used to indicate the Ro value) films with different Si implantation doses. In both doses, two clear emission bands, band A (1.9 eV) and band B (2.4 eV), were observed in the as-implanted films. Another small band at about 2.8 eV (Band C) can also be observed. As Ro decreases or Si implantation dose increases, the intensity of these bands will decrease, namely, the emission intensity decreases with increasing excess Si concentration in SRO films. It is noted that the as-deposited SRO films without Si implantation do not present obvious emission.

Figure 2 shows the annealing effect on the implanted SRO films. For all the SRO films used in this study, all the emission bands that appear in the as-implanted state, namely, band A, band B and band C vanish after thermal annealing at 1100°C. However, a new emission band that is located around 1.7 eV appears after annealing. The intensity of this band depends on the Ro, Si implantation dose, and annealing time. With the decrease of Ro (or increase of Si excess), the intensity decreases. The annealing time is critical to the intensity. An optimum annealing time of 60 minutes exists to obtain highest emission intensity. Both shorter and longer annealing time will decrease the intensity. Meanwhile, a small blue shift in peak position can be observed after thermal annealing, as shown in Figure 3. It is also noted that with the increase of Ro, the emission peak shows a slight blue shift as depicted in Figure 3. The emission intensity is higher for SRO_{20} and SRO_{30} films as the Si implantation dose increases when annealed during 60 minutes. This is not the case for SRO_{10} film.

3.2 Photoluminescence of SNO films

Figure 4 shows the PL spectra of as-deposited SNO films. Being different to SRO, the SNO films show strong luminescence in the as-deposited state. These films present similar emission band at around 2.38-2.66 eV and the peak position shows a blue shift as the Si excess decreases or nitrogen (N) concentration increases, as shown in Figure 7, meanwhile, the emission intensity also increases.

Thermal annealing has quite different effect on the emission of the SNO films with different Si and N content. Figures 5 and 6 show the variation of PL band of two SNO samples with different Si and N content, sample M1 and M3, respectively. After annealing, both samples always emit with a small blue shift as increasing annealing time, also shown in Figure 7. However, for sample M1 that has lower Si concentration and higher N concentration, the emission intensity decreases as the annealing time increases; on the other hand, for sample M3 that has higher Si concentration and lower N concentration compared with M1, the intensity increases with annealing time until a critical time of 90 min. The intensity will decrease when annealing time is longer than 90 minutes. Similar behavior was observed for samples M2 and M4.

The SRO and SNO films present very different PL properties. The as-deposited SRO films present very weak emission. After Si implantation and thermal annealing, an emission band at 1.7 eV was observed. However, the SNO films present strong emission in 2.38-2.66 eV, both in the

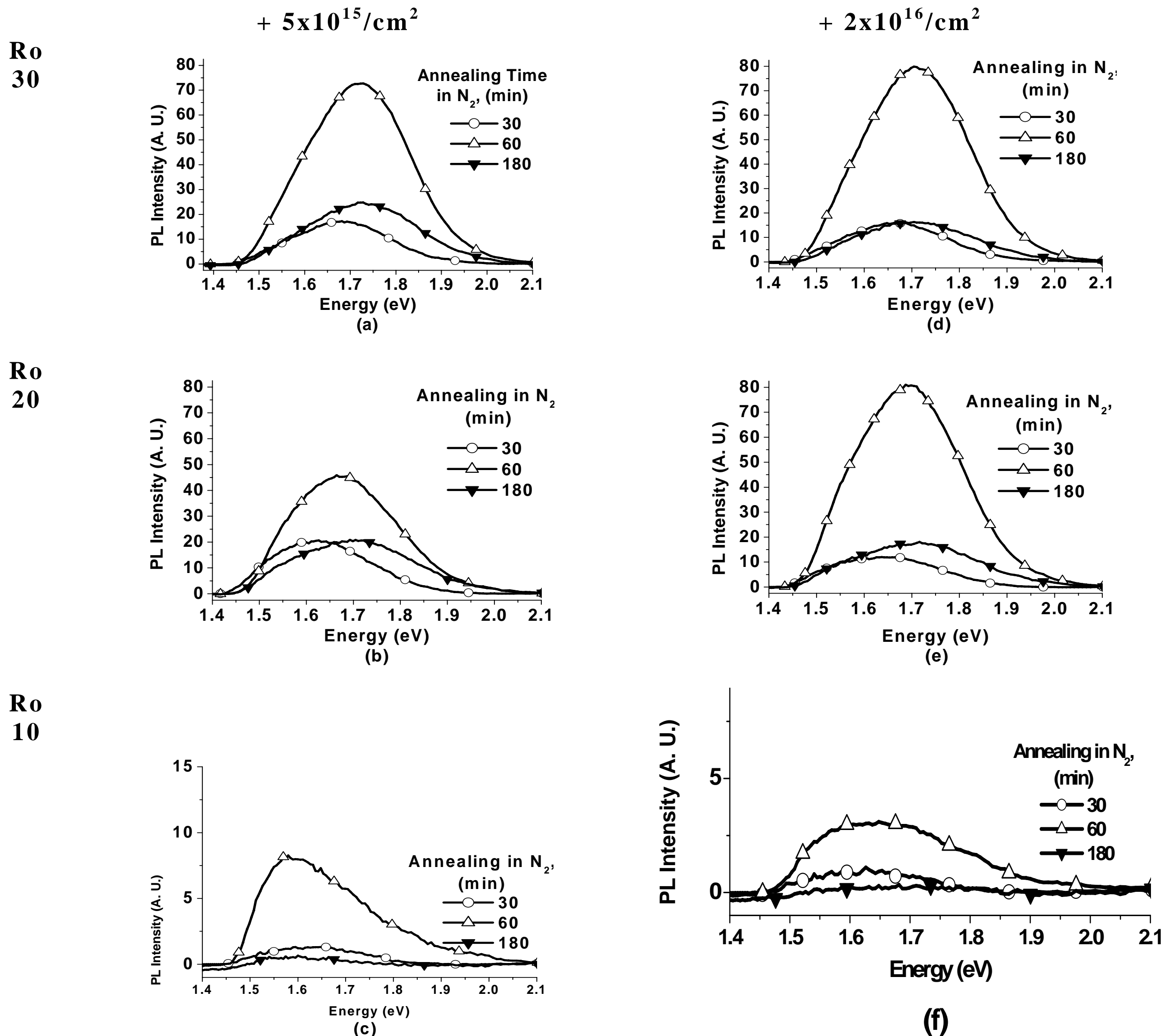

Figure 2. PL spectra of the implanted LPCVD-SRO films with different annealing time and Ro (10, 20 and 30).

as-deposited and annealed samples. By optimizing the preparation parameters of the SNO films, the intensity of this blue emission (500 nm) could be stronger.

4. Discussion

The as-deposited SRO films show very weak PL intensity, while the Si implantation makes the PL intensity increase largely. This indicates that the three emission bands (A, B, C) are correlated with Si implantation. The emission band A (peak 1.9 eV) has been also observed in porous silicon and has been ascribed to the non-bridging oxygen hole centers (NBOHC) [9]. The emission band C (peak 2.7-2.8 eV) has been considered to be due to the Si-implantation created neutral oxygen vacancies [10]. The band B (peak 2.4 eV) has been ascribed to the geminate recombination within localized band tail states excited below the optical band gap in SiO_x (x<2), or due to the hydrogen-related species [11, 12].

When the SRO films are annealed at high temperature (1100°C), the structural properties of the SRO films will be modified. Structural and optical measurements have shown that the SRO films contain large partial of sub-stoichiometric SiO_x (x<2) phase. However after annealing, the sub-stoichiometric phase will separate into the stoichiometric SiO_2 and Si nanoclusters. Thus the NBOHC and neutral oxygen vacancies will reduce as function of annealing time and the corresponding emission peaks (band A and C) will be modified. The band B is related to the band tail states or hydrogen-related species, then it will also be eliminated after the amorphous Si nanoclusters crystallized in high temperature annealing process.

There is a large amount of reports about the Si nanoclusters' emission. The peak position of the emission will shift according to the excess Si concentration in the material. This emission has been related to the radiative recombination of photogenerated carriers in the Si nanoclusters [10, 13, 14]. This study shows that the peak

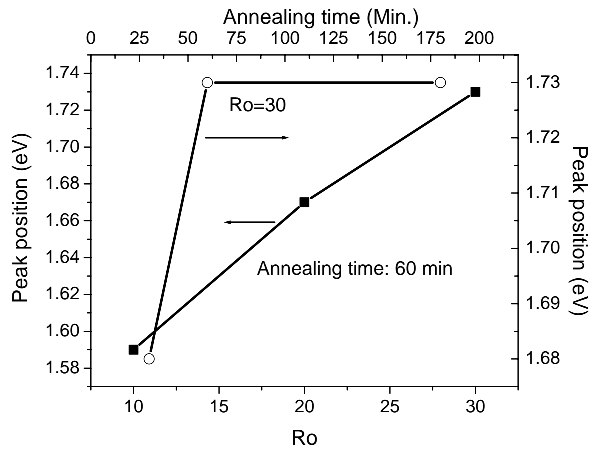

Figure 3. Emission peak position as function of Ro and thermal annealing time of the SRO films.

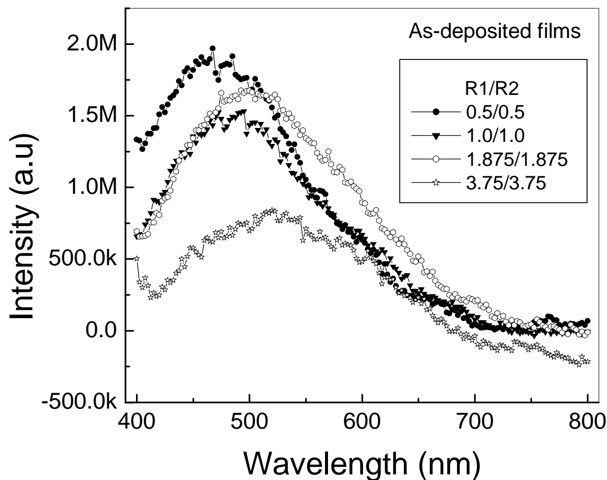

Figure 4. PL spectra of the as-deposited SNO films with different Si and N content. An emission band around 2.38-2.66 eV was presented for all samples.

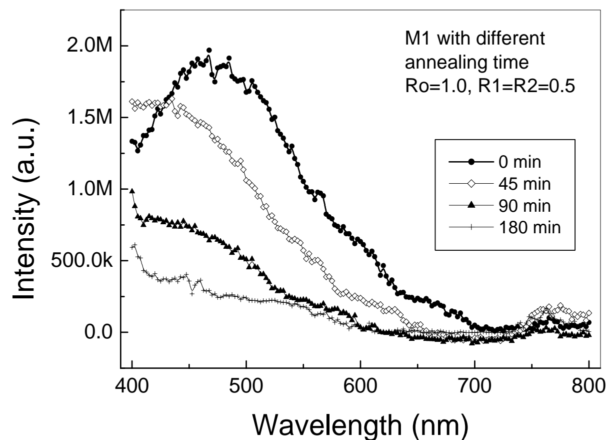

Figure 5. PL spectra of sample M1 with different thermal annealing duration. The intensity decreases when thermal annealing duration increases. Sample M1 has comparatively less Si content and more Nitrogen content.

position of our samples shifts according to the excess Si and thermal annealing time, as shown in Fig.3. A clear blue shift can be observed as Ro increases (Si excess decrease) or annealing time increases. It is expected that the average

diameter of Si nanocrystals will decrease with the decrease of Si excess. However, the diameter of the Si nanocrystals will increase with annealing time. If the band-to-band emission dominates the PL process in our sample, a red-shift in peak position should be observed with increasing annealing time. This is not the case of this experiment. Therefore, the experimental results in this study exclude the possibility of band-to-band emission of the Si nanocrystals. In fact, when the Si nanocrystals are very small, the Si/SiO_2 interface will play important role. Due to the large stress in the Si/SiO_2 interface, localized states will form in the band gap of the Si nanocrystals [15]. And the photogenerated carriers will be trapped by these localized states and then recombine. The Si excess concentration of the SRO samples used in this study is in the range of 1-6% for Ro=20 and 30. TEM study has shown that the average size of the Si nanocrystals in these kinds of SRO films will be smaller than 2 nm [16]. According to the calculation [15], the band gap of the Si nanocrystals of this size should be around 3 eV. However, the measured PL emission has a peak around 1.7 eV. This is an evidence that the PL emission is not via band-to-band recombination. Thus the emission via the localized states is the most possible mechanism. The bonding situation of Si at the Si/SiO_2 interface will change in the thermal annealing process and Si nanocrystals' diameters, thus modifying the energy level of the localized states, resulting in the blue shift of the emission peak with annealing time.

For SNO films, the emission appears at around 2.6 eV, and the emission peak has a red shift with increasing R1 (and thus an increase of excess Si and decrease of N). Our previous research showed that comparable emission band at 2.7 eV was also presented in Si-implanted and annealed SRO films prepared by plasma enhanced chemical vapor deposition technique (PECVD-SRO) with lower Si excess [10, 17]. The emissions from PECVD-SRO and LPCVD-SNO probably have same mechanism due to the same emission position. Another important factor is that the composition of PECVD-SRO and LPCVD-SNO is probably similar. Of course, LPCVD-SNO contains Si, N, and O. And in PECVD-SRO, the compositions of Si, N, and O have also been evidenced [14]. However, the LPCVD-SRO only contains negligible N. The introduction of N into the SNO films probably modifies the structure of the films. One possible modification is that the segregation of excess Si into large nanocrystals will be more difficult and the average size of the Si nanocrystals will be limited to a small value. In this case, a higher annealing temperature (>1000°C) is required for the segregation of larger Si nanocrystals. F. Iacona *et al* have used annealing temperature as high as 1250°C in order to get strong PL intensity in PECVD-SRO films that contains N [14]. Their study showed that for PECVD-SRO with similar excess Si

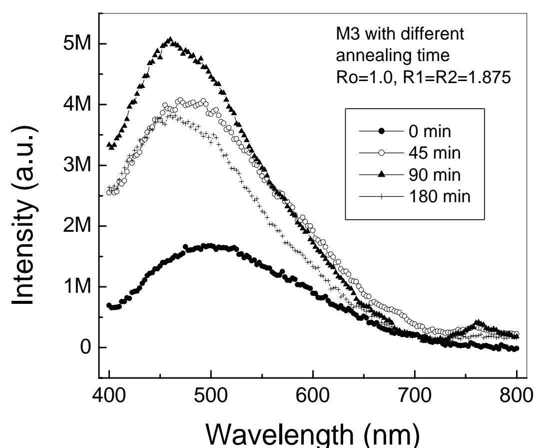

Figure 6. PL spectra of sample M3 at different thermal annealing time. The emission intensity increases when thermal annealing duration increases until an optimum value, 90 minutes, is reached. The intensity decreases again for annealing time longer than 90 minutes. Sample M3 has comparatively more Si content and less Nitrogen content.

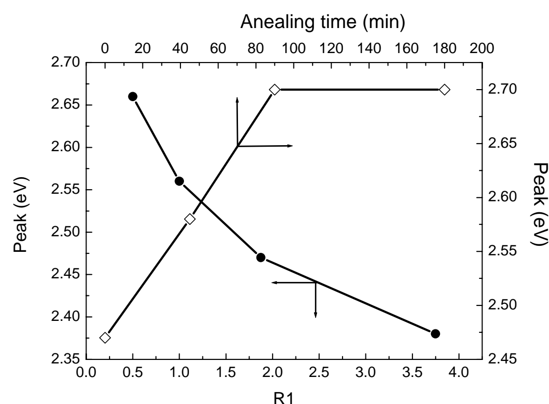

Figure 7. Emission peak position as function of R1 and thermal annealing time of the SNO films.

concentration as that of the samples used in this study, very obvious red shift with annealing temperature was observed.

Therefore, the emission of SNO at larger energy compared with that of SRO is possibly due to the small Si nanocrystals formed in SNO films under the experimental condition used in this study. The blue shift in peak position with decreasing R1 and increasing annealing time can also be explained considering the average Si nanocrystals' size and Si/SiO_2 interface states, as discussed for SRO films. It is possible that in as-deposited SNO films, the excess Si has already formed nanocrystals (or amorphous nanoclusters) due to the existence of N, this is the reason that obvious emission can be observed in as-deposited SNO films. From this point of view, N plays similar role as Si implantation into SRO. It has been shown that the sudden enhancement in PL by the Si-implantation in SRO could be due to the distruction of the large Si segregations in the as deposited SRO films, and thus to increase of the density of small Si nanocrystals [18].

5. Conclusions

We have studied the photoluminescence properties of LPCVD SRO and SNO films. They present very different PL spectra. Only after Si-implantation and thermal annealing, the SRO films present strong red-light emission (1.7 eV or 730 nm). However, the as-deposited SNO films present strong blue-light emission (around 2.6 eV or 500 nm). The emission intensity could be even enhanced by thermal annealing for some SNO films. An explanation of the experimental results was presented. It is suggested that N plays an essential role in the modification of the emission process.

Acknowledgements

The authors appreciate to Pablo Alarcon for the sample preparation. This work is supported by CONACYT, Mexico.

References

[1] M.Aceves, W.Calleja, C. Falcony, J.A. Reynoso-Hernandez, Revista Quimica Analitica. **18**, 5 (1999).
[2] F.Flores, M.Aceves, J.Carrillo, C.Dominguez, C.Falcony, Revista Mexicna de Fisica. **47**, 267 (2001).
[3] Shimizu-Iwayama T., Yoichi T., Atsushi K., Motonori T., Setsuo N., Kazuo S., Thin Solid Films. **276**, 104 (1996).
[4] Rebohle L., Von Borany J., Grotzchel R., Markwitz A., Schmidt B., Tyshenko I.E., Skorupa W., Frob H., Leo K., Phys. Stat. Sol.(a). **165**, 31 (1998).
[5] Ossicini S., Phys. Stat. Sol.(a). **170**, 377 (1998).
[6] Kenyon A.J., Trwoga P.F., Pitt C.W., Rehm G., J. Appl. Phys. **79**, 12 (1996).
[7] P.Temple-Boyer, B.Hajja, J.L.Alay, J.R.Morante, A.Martinez, Sensors and Actuators. **74**, 52 (1999).
[8] A.E.Kuiper, S.W.Koo, F.H.P.M.Habraken, and Y.Tamminga, J.Vac. Sci. Technol. B. **1**, 62 (1982).
[9] S.M.Prokes, IEEE J. Selected Topics in Quantum Electronics. **1**, 1140 (1995).
[10] Francisco Flores-Gracia, Ph.D. Thesis, INAOE, Puebla, Dec. (2001).
[11] B.H.Augustine, Y.Z.Hu, E.A.Irene and L.E.Mcneil, Appl. Phys. Lett. **67**, 3694 (1995).
[12] Y.D.Glinka, S.H.Lin, Y.T.Chen, Appl. Phys. Lett. **75**, 778 (1999).
[13] T.Shimizu-Iwayama, N.Kurumado, J. Appl. Phys., **83**, 6018 (1998).
[14] F.Iacona, G.Franzo, C.Spinella, J. Appl. Phys., **87**, 1295 (2000).
[15] M.V.Wolkin, J.Jorne, P.M.Faucher, Phys. Rev. Lett., **82**, 197 (1999).

[16] D.J.DiMaria, J.R.Kirtley, E.J.Pakulis, D.W.Dong, T.S.Kuan, F.L.Pesavento, T.N.Theis, J.A.Cutro, S.D.Brorson, J. Appl. Phys. **56**, 401 (1984).

[17] M.Aceves, F.Flores, J.Carrillo, C.Dominguez, C.Falcony, Proceedings of 9th Annual Intl. Conf. on Composites Engineering, San Diego, California. July, 2002, p11. Francisco Flores-Gracia, Ph.D. Thesis, INAOE, Puebla, Dec. 2001.

[18] Kim TG; Whang CN; Sun Y; Seo SY; Shin JH; Song JH, J. Appl. Phys. **91**, 3236 (2002).